The effect of docetaxel on retinal pigment epithelial cells

Jialin Li [a,d,1], Xiao Liu [b,e,1], Qiaohui Yang [a,f], Jian Huang [a,f], Wang Zhou [a], Zhirong Tan [c], Zhuo Li [b,e,2,*], Di Zhou [a,d,**]

[a] NHC Key Laboratory of Human Stem and Reproductive Engineering, School of Basic Medical Science, Central South University, Changsha, China
[b] Department of Ophthalmology, The Second Xiangya Hospital, Central South University, Changsha, China
[c] Department of Clinical Pharmacology, Xiangya Hospital, Central South University, China
[d] Hunan International Scientific and Technological Cooperation base of Development and Carcinogenesis, Changsha, China
[e] Hunan Clinical Research Center of Ophthalmic Disease, Changsha, China
[f] Reproductive and Genetic Hospital of CITIC-Xiangya, Changsha, China

ARTICLE INFO

ABSTRACT

Docetaxel (DTX) is a highly effective anti-tumor drug frequently used in clinical practice. Previous reports indicated that complications after DTX therapy could be related to retinal pigment epithelial (RPE) cell dysfunction, although no direct reports of this relationship have been published. In this study, human embryonic stem cell–derived RPE (hESC-RPE) cells were used to explore the effects of DTX on their morphology, viability, apoptosis, proliferation, and cell cycle. We also searched for DTX residue in these cells. DTX had a time- and concentration-dependent inhibitory effect on hESC-RPE cell viability, and the cells only survived after 24 h of stimulation with 0.1 mg/mL of DTX. Following drug withdrawal, the cell morphology continued to change, and hESC-RPE cell damage was observed. High-performance liquid chromatography/mass spectrometry showed that some unmetabolized DTX remained in hESC-RPE cells after the 48 and 120 h DTX treatments. Flow cytometry and immunofluorescence revealed that DTX significantly enhanced apoptosis, and the Cell Counting Kit-8 assay and flow cytometry indicated that DTX inhibited cell proliferation and blocked the cell cycle. These results suggest that DTX has a direct cytotoxic effect on hESC-RPE cells. Thus, RPE cell damage after DTX treatment may present an important safety problem that could potentially limit the application of this drug in clinical practice. The findings of this study suggest that clinicians should weigh the benefits of DTX versus the risks of ocular adverse reactions rationally. Timely diagnostic evaluation and drug withdrawal will be conducive to the recovery of patients' visual acuity.

1. Introduction

Angiogenesis plays an important role in the growth, invasion, and metastasis of malignant tumors [8,34]. Therefore, inhibiting tumor angiogenesis is an effective strategy for tumor treatment. Since the important role of angiogenesis in tumor growth and metastasis was first proposed in 1971 [13], anti-tumor angiogenesis has become a hotspot of research. Docetaxel (DTX), belonging to the taxane family, is a very effective and widely used antitumor drug with anti-angiogenic effects. DTX alone, or combined with other drugs, has considerable efficacy in treating many types of solid tumors [24,3,7]. In addition, DTX is more easily obtained than paclitaxel, the first drug used in the treatment of metastatic hereditary breast cancer, and has a better effect in inducing apoptosis of some tumor cells, including metastatic breast cancer refractory to paclitaxel [17].

However, treatment of tumors with DTX has side effects. Previous case studies have reported canalicular stenosis [12], conjunctivitis, and punctual stenosis [26] in metastatic breast cancer patients treated with DTX. These ocular adverse reactions may be caused by the secretion of DTX in tear film leading to tubular fibrosis after direct contact with the

ocular surface and canal system. Moreover, a study has shown that DTX can be detected in tear samples after intravenous injection [11]. Additionally, gemcitabine combined with DTX for treating stage IV sarcoma caused severe uveal effusion in the right eye, and in the left eye, it ruptured the ellipsoid zone in the photoreceptor inner segment and the choroid [19]. Thus, DTX monotherapy or combination therapy with gemcitabine may cause visual manifestations. Other studies have shown that DTX can cause peripheral edema and pleural effusion through a capillary leak syndrome–like mechanism. Uveal effusion and outer retinal wall rupture caused by DTX monotherapy may also occur through this mechanism. Cystoid macular edema (CME) is also a known complication of DTX chemotherapy [30], and it can be diagnosed via fluorescein angiography or optical coherence tomography, where fluid accumulation in multiple cyst-like spaces is observed in the macula [18]. Several clinical cases have reported taxane-induced CME [10,20,21,31, 33,9]. In one of these cases, a patient without retinopathy who had received hydroxychloroquine for rheumatoid arthritis for 33 years developed bilateral vision loss after receiving DTX chemotherapy for breast cancer. Optical coherence tomography showed bilateral cystic macular disease, and fluorescein angiography showed no signs of leakage. An impaired transcellular retinal pigment epithelium was suggested as a possible cause for nonleaking CME [9]. Similarly, in another study, paclitaxel therapy showed a toxic effect on microtubules, resulting in the obstruction of retinal pigment epithelial (RPE)–dependent microtubule fluid absorption [20]. A report of bilateral CME after DTX chemotherapy also supported the possibility that RPE dysfunction may be the mechanism triggering or compounding the taxane effect [10]. DTX, which is administered intravenously, can reach cancer cells in the bloodstream but also affect healthy cells in the body, including those in the eye. However, there have been no direct reports on the toxic effects of DTX on healthy retinal pigment epithelial cells in vitro.

RPE cells are very important blood-retinal barrier cells. They express various RPE-specific proteins and secrete growth factors that support other cell types in the eyes. To test whether DTX can directly damage RPE cells, this study was designed to investigate the effects of DTX using hESC-RPE cells as a cell culture model. DTX residue was detected using high-performance liquid chromatography/mass spectrometry (HPLC/MS/MS) technology after the viability of hESC-RPE cells treated with DTX was examined. Apoptosis, proliferation, and cell cycle distribution were also evaluated in these cells following DTX administration. Taken together, our study aims to demonstrate that DTX has a direct cytotoxic effect on hESC-RPE cells.

2. Materials and methods

2.1. Cell culture and differentiation

Human embryonic stem cell line 90 cells (i.e., hESC-90; Human Embryonic Stem Cell Bank at the National Engineering and Research Center of Human Stem Cells, Changsha, China) were maintained on hESC-qualified Matrigel (Corning, NY, USA) in mTeSR1 medium (STEMCELL, Vancouver, BC, Canada). Before induction, the human embryonic stem cells (hESCs) were dissociated and cultured in Aggre-Well™ 400 plates at 2×10^5 cells/cm^2 overnight to form embryoid bodies (EB). The cell culture medium was replaced with EB medium consisting of Dulbecco's Modified Eagle Medium/Ham's nutrient mixture F-12 (i.e., DMEM/F12; Thermo Fisher Scientific, Waltham, MA, USA), 1% nonessential amino acids, 0.1 mM 2-mercaptoethanol (Thermo Fisher Scientific), and 15% knockout serum replacement (i. e., KOSR; Thermo Scientific).

We defined EB formation as differentiation day 0. From day 0–7, EBs were cultured in suspension in EB medium supplemented with 1 μM dorsomorphin and 5 μM SB431542 (STEMCELL). Thereafter, the cytokine added to the EB medium was changed to 10 μM nicotinamide (Sigma-Aldrich, St. Louis, MO, USA) for adherent induction from day 7–35. 10 ng/mL activin A (R&D Systems, Minneapolis, MN, USA) was

Table 1
qRT-PCR primer sequences for human genes.

Primer name	Forward sequence	Reverse sequence
ACTB	TCCCTGGAGAAGAGCTACGA	AGCACTGTGTTGGCGTACAG
BEST1	GGACTGCAGCCAGTGAAACT	CCTTGCTCGTCCTTGCCTTC
RPE65	GCATCCTGCTGGTGGTTACA	TTGCCCATCAAACAGGTGGT
TYR	GCACAGATGAGTACATGGGAGG	CTGATGGCTGTTGTACTCCTCC
MITF	TTCACGAGCGTCCTGTATGCAGAT	AGTTTCCCGAGACAGGCAACGTAT
OCT4	AGCGAACCAGTATCGAGAAC	TTACAGAACCACACTCGGAC
NANOG	AAGGTCCCGGTCAAGAAACAG	CTTCTGCGTCACACCATTGC

Abbreviations: *ACTB*, Actin Beta; *BEST1*, Bestrophin-1; *RPE65*, Retinal Pigment Epithelium-Specific Protein 65 kDa; *TYR*, Tyrosinase; *MITF*, Melanocyte Inducing Transcription Factor; *OCT4*, POU Class 5 Homeobox 1; *NANOG*, Nanog Homeobox.

added from days 14–28. On the 35th day after induction, a large number of RPE precursors were harvested. We mechanically uprooted non-RPE precursors, digested the remaining cells, and expanded them with X-VIVO10 medium (Lonza, Walkersville, MD, USA) to obtain RPE cells.

2.2. Immunofluorescence

Cells were fixed in 4% paraformaldehyde solution (i.e., PFA; Bosterbio, Pleasanton, CA, USA) for 10 min at 4 °C, followed by permeabilization with 0.2% Triton X-100 (Solarbio, Beijing, China) in 1× phosphate-buffered saline (PBS) for 15 min and blocked with 10% normal donkey serum (Jackson ImmunoResearch, Tucker, GA, USA) for 1 h at room temperature. The cells were incubated with primary antibodies against Retinal Pigment Epithelium-Specific Protein 65 kDa (*RPE65*; 1:200, ab235950) and Melanocyte Inducing Transcription Factor (*MITF*; 1:200, ab122982) (Abcam, Cambridge, UK) at 4 °C overnight, and subsequently with Alexa Fluor594-conjugated secondary antibodies and Alexa Fluor488-conjugated secondary antibodies (1:1000, Life Technologies, Carlsbad, CA, USA) for 1 h at room temperature. Cell nuclei were labeled with DAPI (ChemCruz, Dallas, TX, USA) for 10 min at room temperature. After a brief wash with PBS, the cells were viewed, and images were taken using an inverted fluorescence microscope.

2.3. Quantitative real-time polymerase chain reaction (qRT-PCR)

Total RNA was isolated from cells using TRIzol (Sigma-Aldrich) following the manufacturer's instructions; then, 1 μg of total RNA was reverse-transcribed into complementary DNA (cDNA) using the Evo M-MLV RT Kit (Accurate Biology, Changsha, China). qRT-PCR was performed using a LightCycler® 480 SYBR Green I Master (Roche, Mannheim, Germany). Table 1 lists the primer sequences (Sangon Biotech, Shanghai, China). The Actin Beta (*ACTB*) gene was used as a housekeeping gene to quantify the levels of cDNA expression per sample, and relative fold changes were calculated using the $2^{-\Delta\Delta Ct}$ method.

2.4. Trypan blue assay

hESC-RPE cells were grown in 24 well plates at 200,000 cells/well and incubated at 37 °C and 5% CO$_2$. After 24 h, the cells were treated with DTX injections (Qilu Pharmaceutica, Jinan, China) at four concentrations (0.1, 0.3, 0.5, and 0.7 mg/mL) for 24, 48, and 72 h. The control cells (without DTX) were treated in the same manner. Cell viability was evaluated by 0.4% trypan blue (Thermo Fisher Scientific) staining using a hemocytometer and an optical microscope. Living cells repel trypan blue as their membrane structure is intact, while dead cells stain blue owing to increased membrane permeability. Cell survival (%) was calculated as the ratio of the number of living cells divided by the total number of cells.
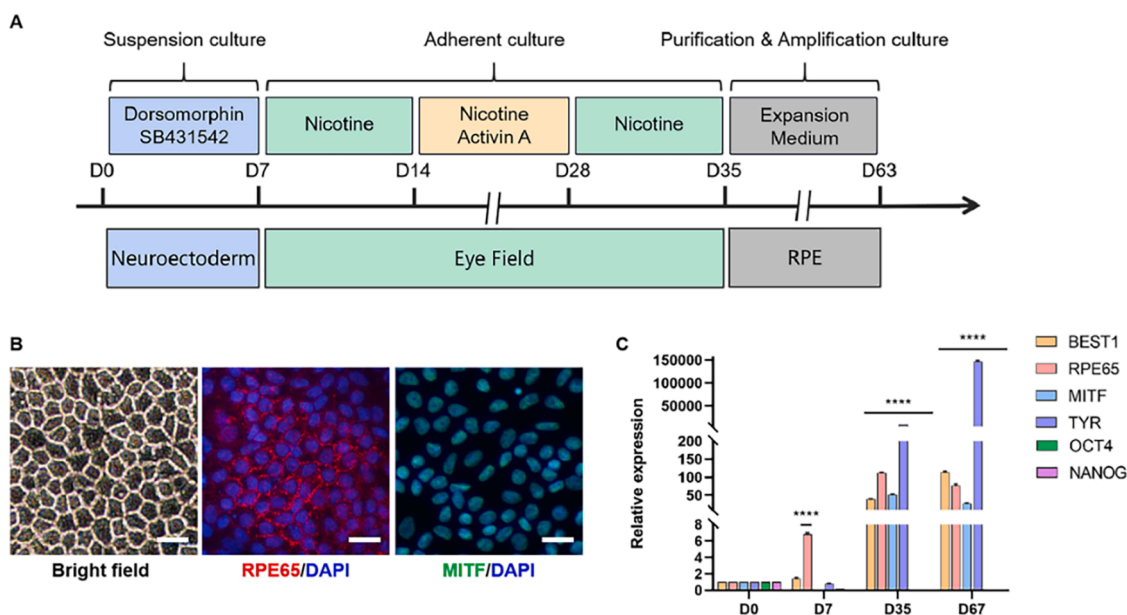
Fig. 1. Characterization of RPE cells derived from hESC. (A) A schematic illustration of directional differentiation of hESCs into RPE cells. (B) Immunofluorescence staining of hESC-RPE showing *RPE65* and *MITF* expression. (C) Quantitative real-time PCR analysis of the RPE markers. Gene expression levels were normalized to *ACTB* and presented relative to the hESCs expression levels on differentiation day (D) 0. ****$P < 0.0001$ compared with D0. Abbreviations: RPE, retinal pigment epithelial; hESC, human embryonic stem cells; *BEST1*, Bestrophin-1; *RPE65*, Retinal Pigment Epithelium-Specific Protein 65 kDa; *TYR*, Tyrosinase; *MITF*, Melanocyte Inducing Transcription Factor; *OCT4*, POU Class 5 Homeobox 1; *ACTB*, Actin Beta.

2.5. DTX residue detection

Cells (200,000 cells/well) were placed in a 24-well plate and cultured for another week at 100% confluency. Thereafter, 0.125 mg/mL of DTX was added as a stimulant at 48, 72, 96, and 120 h. The cells were washed with double-distilled water three times and collected in a centrifuge tube for ultrasonic crushing for 15 min. The final samples were sent to the Institute of Clinical Pharmacology of Central South University for HPLC-MS/MS detection of DTX residue. Briefly, the standard stock solution of DTX, 0.552 mg/mL, was diluted with methanol/water (1:1, v/v) to prepare a set of DTX calibration solutions with various concentrations and then deproteinized with acetonitrile. After centrifugation at 15,000 rpm for 10 min at 4 °C, 100 μL of the supernatant was used for HPLC-MS/MS analysis to establish the standard curve. Tested samples were also diluted with methanol/water (1:1, v/v) and deproteinized by addition of acetonitrile. Analyses were performed after centrifugation as above. All chromatography experiments were performed at ambient temperature using the Nexera UHPLC/HPLC system (Shimadzu, Japan). The QTRAP 6500 mass spectrometer produced by AB Sciex (Concord, ON, Canada) was used for analyte detection and operated in the positive ion mode using multiple reaction monitoring. The precursor-product ion transitions were monitored at m/z 830.3→549.2 for DTX.

2.6. Hoechst 33258 staining

When the cells were in the logarithmic growth phase, DTX was added to the culture at 0, 0.075, 0.100, and 0.125 mg/mL for 24 h. Apoptotic cells were detected using Hoechst 33342 staining (1:1000, Thermo Scientific). Cells were washed three times using PBS after drug stimulation and fixed in 4% paraformaldehyde at 4 °C for 15 min. After three washes with PBS, cells were stained with Hoechst 33258 for 5 min and were further washed three times using PBS. Finally, nuclear changes were observed using a fluorescence microscope.

2.7. Cell apoptosis assay

Apoptosis was determined using an Annexin V Apoptosis Detection Kit (Sangon Biotech). The cells were cultured in 12-well plates at 2×10^5 cells/well. After 24 h of DTX stimulation (0, 0.075, 0.100, and 0.125 mg/mL), the treated cells were collected and washed three times with cold PBS. The cells were resuspended in 195 μL annexin-binding buffer and incubated with 5 μL Annexin V-FITC for 5 min at room temperature in the dark. Afterward, the cells were washed and labeled with 10 μL propidium iodide (PI) in 190 μL annexin-binding buffer. The cell suspensions were analyzed using a BD Accuri C6 flow cytometer (BD Biosciences, Franklin Lakes, NJ, USA).

2.8. Cell proliferation assay

Cell proliferation was assessed using the Cell Counting Kit-8 assay (CCK8; Sangon Biotech). The cell suspension was prepared and adjusted to 2×10^5 cell/mL with medium and seeded into 96-well plates at 2×10^4 cells in 100 μL medium per well. After 48 h, DTX (0, 0.075, 0.100, and 0.125 mg/mL) was added, and the cells were incubated for 24 h. Five replicate wells were assigned per experimental group, including the group without DTX. Each well received 10 μL CCK8 and was incubated for 3 h. The absorbance was measured at 450 nm using a microplate reader (Thermo Fisher Scientific).

2.9. Cell cycle analysis

Cell cycle was evaluated using a Cell Cycle Analysis Kit (4 A BIOTECH, Beijing, China). The cells were seeded onto 24-well plates at 5×10^5 cells/well, then treated with DTX at 0, 0.075, 0.100, and 0.125 mg/mL for 24 h. The PI staining solution containing RNase was prepared in advance following the manufacturer's instructions. Overnight fixed cells were collected, washed with ice-cold PBS for 3 times and then add RNase-PI solution as per standardize protocol [5,6]. The cells were incubated for 30 min at 37 °C in the dark, and the stained samples were analyzed using a BD Accuri C6 cytometer.
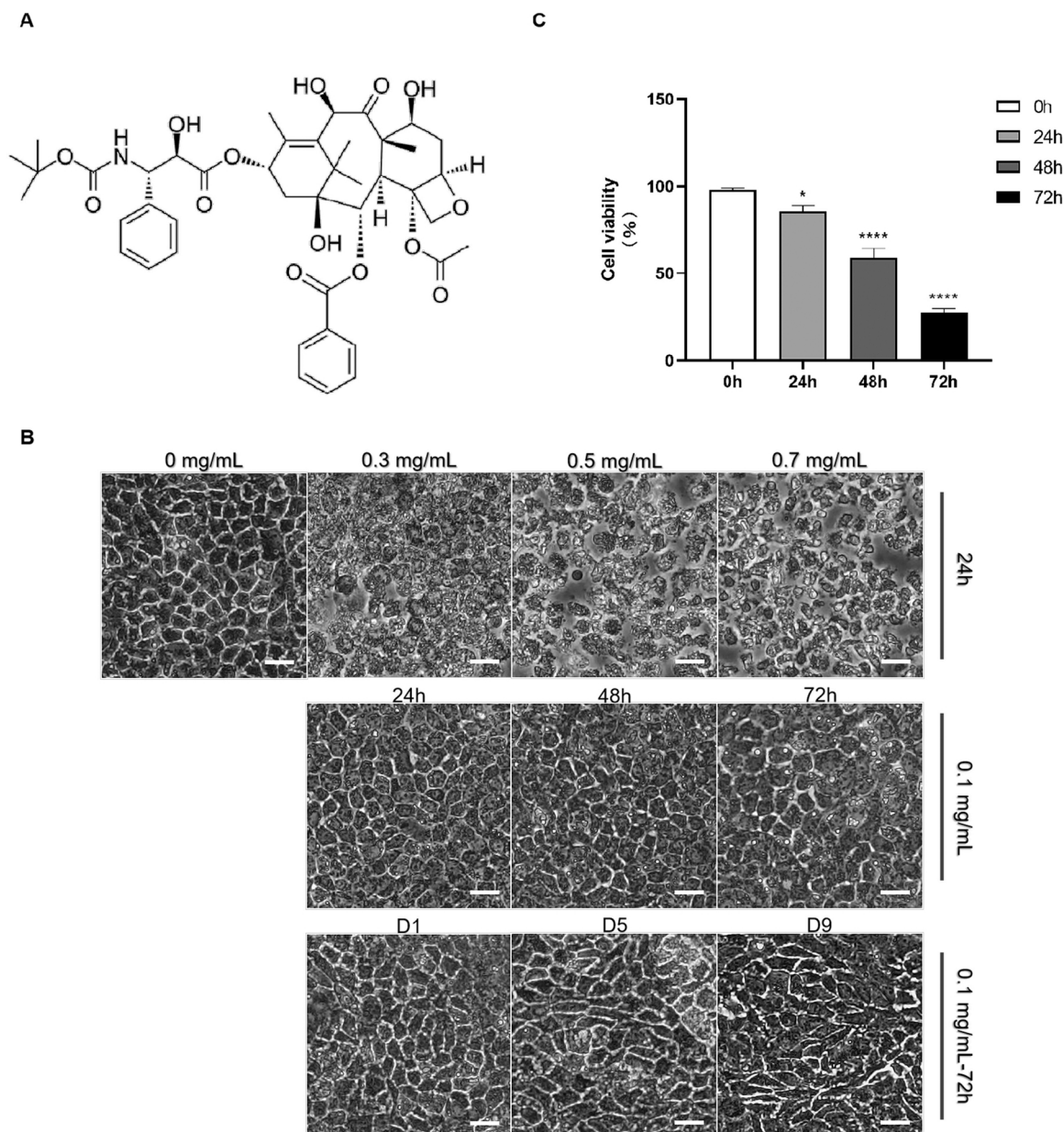
Fig. 2. Effect of DTX on hESC-RPE cells. (A) Chemical structure of DTX. (B) Morphological observations of hESC-RPE cells treated with various DTX concentrations for 24 h (top row) and 0.1 mg/mL of DTX over time (middle row). Cells stimulated with 0.1 mg/mL of DTX for 72 h were cultured in fresh amplification medium (bottom row). (C) Cell viability was assessed using trypan blue staining. *$P < 0.05$ and ****$P < 0.0001$. Abbreviations: DTX, docetaxel; hESC-RPE, human embryonic stem cell derived retinal pigment epithelial.

2.10. Statistical analyses

All experiments were independently repeated at least three times. Quantitative data were expressed as means ± standard error of the mean. Statistical analyses were performed using Prism 8 software (GraphPad Software, La Jolla, CA, USA). Student's t-test was used to compare two groups, whereas one-way analysis of variance with Tukey's post-hoc test was performed for multiple comparisons. P-values of < 0.05 were considered statistically significant.

3. Results

3.1. Differentiation of hESCs into RPE cells

We induced the differentiation of hESCs into RPE cells using an established protocol (Fig. 1A). After nine weeks of spontaneous differentiation, artificial isolation, purification, and amplification, the hESC-RPE cells exhibited highly similar structural characteristics of primary RPE cells under an optical microscope, including close arrangement and the typical cobblestone shape (Fig. 1B). Additionally, the hESC-RPE cells showed appreciable *RPE65* and *MITF* immuno-staining (Fig. 1B). qRT-PCR analysis showed that RPE-specific markers, such as Bestrophin-1 (*BEST1*), *RPE65*, *MITF*, and Tyrosinase (*TYR*), were highly expressed. Notably, *TYR* expression was 100,000 times higher in the hESC-RPE cells than in the hESCs (Fig. 1C). As expected, stem cell markers, such as *OCT4* and *NANOG*, were highly expressed at the beginning of differentiation, and their expression gradually decreased with time (Fig. 1C). Together, these results suggest a successful commitment of hESCs to RPE cells.
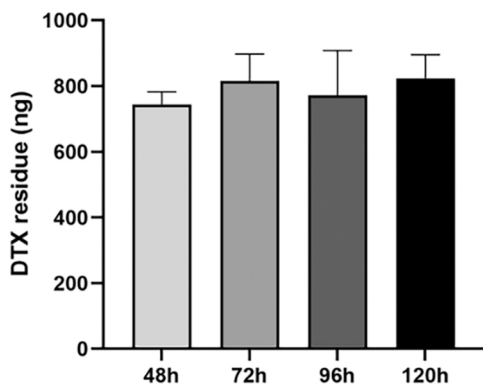
Fig. 3. DTX residue in human embryonic stem cell derived retinal pigment epithelial cells.

3.2. Effects of DTX on cell morphology and viability

Fig. 2A presents the chemical structure of DTX. According to the drug manufacturer's instructions, the final concentration of the DTX mixture after calculating the dosage used by the patient should not exceed 0.74 mg/mL. Before we evaluated the effect of DTX on hESC-RPE cells, we treated RPE cells with various concentrations of DTX. Morphological analysis indicated that all cells died after stimulating with DTX at concentrations of 0.3 mg/mL and higher for 24 h (Fig. 2B); cell death was confirmed by trypan blue staining (data not shown). A few floating or dead cells were observed 24 h after stimulating with 0.1 mg/mL of DTX, and cell viability decreased by 14.4% (Fig. 2B, C). Further, there was a notable decrease in cell motility at 48 h and a more marked decrease at 72 h compared with the control group, and the cell viability decreased in a time-dependent manner, suggesting delayed cytotoxicity of DTX on hESC-RPE cells (Fig. 2C). Thus, the concentration of the DTX injection in hESC-RPE cells for further experiments was 0.1 ± 0.025 mg/mL.

Further, we continued to culture the 72 h 0.1 mg/mL DTX group of cells with fresh amplification medium instead of a drug-containing medium for several days to observe the morphological changes of the cells (Fig. 2B). With increasing culture time, the number of regular honeycomb cells decreased gradually, and some cells elongated. After nine days of culture, some cells remained damaged and irreparable cells and lost their classic hexagonal RPE morphology.
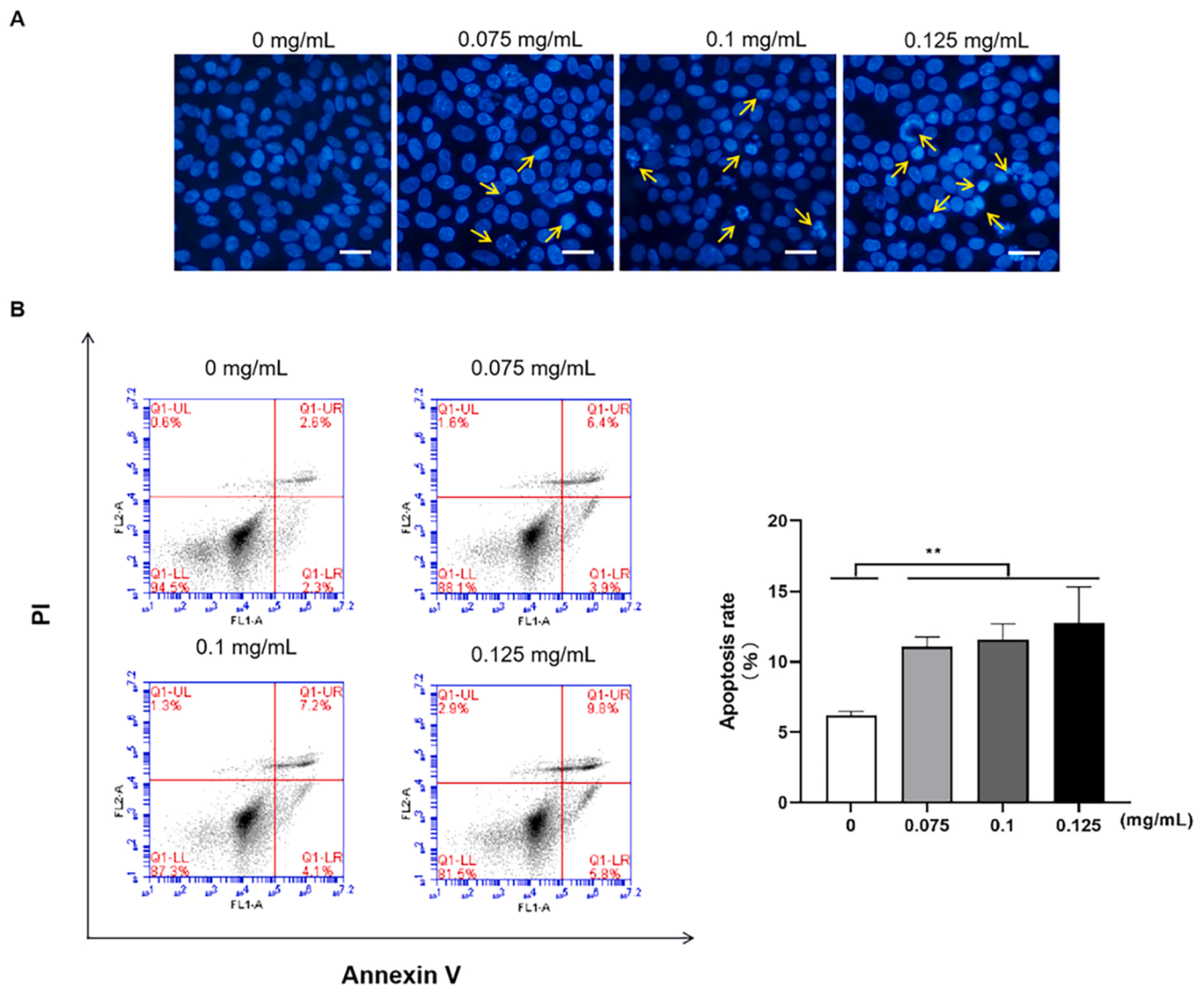

Fig. 4. DTX induces apoptosis in human embryonic stem cell derived retinal pigment epithelial cells. (A) Apoptosis detection by Hoechst 33342 staining. Apoptotic cells are indicated by yellow arrows. Scale bar = 20 μm. (B) Flow cytometry detecting apoptotic cells. Apoptosis percentage = the percentage of early apoptotic cells + the percentage of late apoptotic cells. **$P < 0.01$ compared with control cells. Abbreviations: PI, propidium iodide.
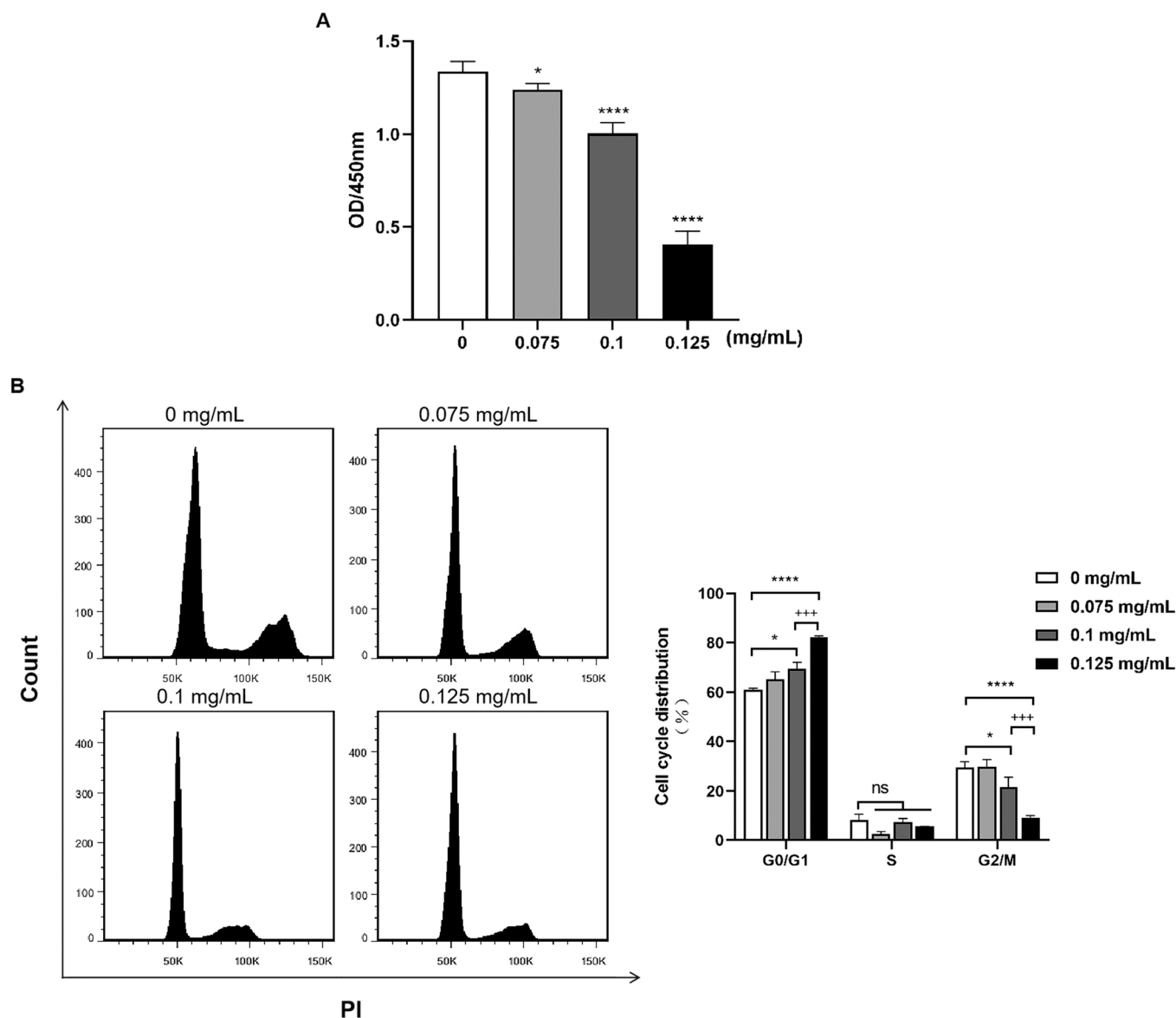
Fig. 5. DTX affects cell proliferation and the cell cycle in human embryonic stem cell derived retinal pigment epithelial cells. (A) Apoptosis detection by Hoechst 33342 staining. Apoptotic cells are indicated by yellow arrows. Scale bar = 20 μm. (B) Cell cycle analysis by flow cytometry. ***$P < 0.01$ compared with control cells; $+++ P < 0.001$ between the 0.100 and 0.125 mg/mL DTX treated groups.

3.3. DTX residue in hESC-RPE cells

After ending drug treatment and returning the cells to normal culture medium without DTX, the cell morphology continued to change, and damaged cells were observed. Therefore, we suspected that the DTX residue in the cells continued to affect cell growth. We used HPLC-MS/MS to detect the DTX residue levels in hESC-RPE cells. After treatment with 0.1 mg/mL DTX for 48–120 h, the DTX residue content ranged from 750 to 820 ng (Fig. 3). The levels did not differ between time points. These results suggested that not only did DTX induced hESC-RPE cell death but the residual DTX in cells also affected cell growth and possibly further impacted cell functions.

3.4. Apoptosis induction by DTX

We next determined whether DTX-induced growth inhibition resulted from cell apoptosis. Hoechst 33342 staining demonstrated that 24 h of treatment with different DTX concentrations changed some morphological features of the hESC-RPE cells, such as nuclear chromatin

condensation and nuclear fragmentation (Fig. 4A), two manifestations of apoptosis. FITC-Annexin V and PI staining followed by flow cytometry detection is often used to distinguish between early and late apoptotic cells and necrotic cells. The results showed that the number of early (PI-negative/Annexin-V-positive) and late (PI-positive/Annexin-V-positive) apoptotic cells significantly increased after treating hESC-RPE cells with 0.075, 0.100, and 0.125 mg/mL of DTX (Fig. 4B). The Hoechst 33342 staining outcomes were consistent with the flow cytometry results.

3.5. Effects of DTX on cell proliferation and the cell cycle

Previous results have demonstrated that DTX can cause apoptosis in hESC-RPE cells. We speculated that DTX also inhibits cell proliferation. Therefore, we performed a CCK8 assay after stimulating hESC-RPE cells with 0.075, 0.100, and 0.125 mg/mL of DTX for 24 h. DTX had an obvious inhibitory effect on hESC-RPE cells, which was more obvious as the concentration increased (Fig. 5A). To determine whether cell proliferation was regulated by the cell cycle, flow cytometry was performed. We found that a low concentration (0.075 mg/mL) of DTX for
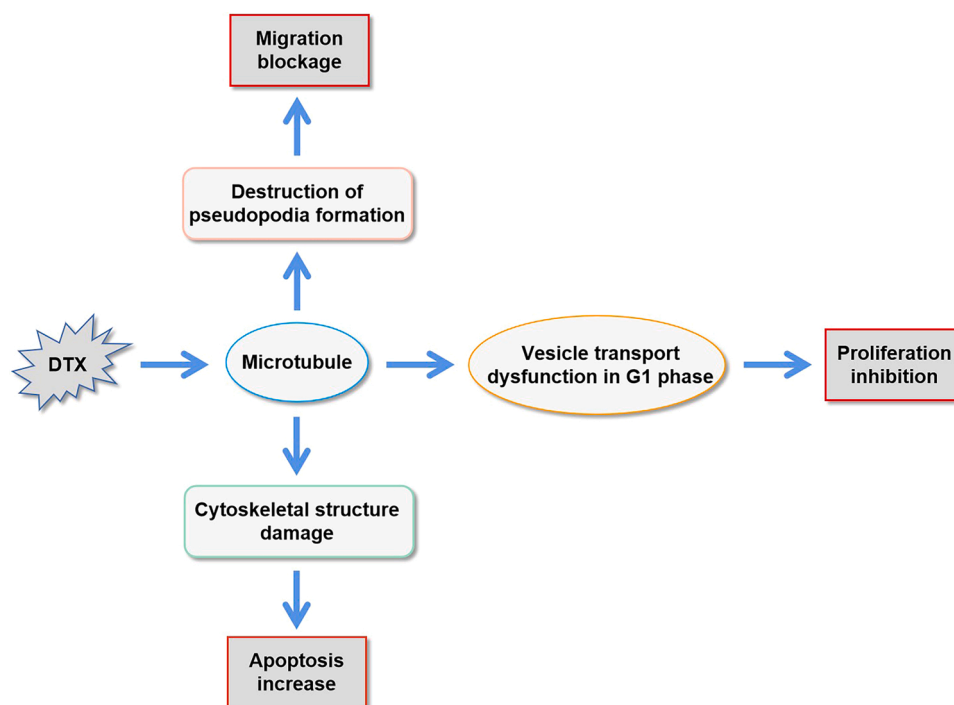
Fig. 6. Diagram of possible mechanism of DTX affecting RPE cells.

24 h did not affect the cell cycle distribution of hESC-RPE cells. However, after 24 h of 0.1 mg/mL DTX stimulation, the proportion of hESC-RPE cells in the G2/M phase significantly reduced, and the proportion of cells entering the G0/G1 phase significantly increased. This effect was more obvious under stimulation with 0.125 mg/mL DTX (Fig. 5B).

4. Discussion

DTX is a front-line standard-of-care anticancer drug. It promotes microtubule polymerization and inhibits depolymerization and spindle formation, inhibiting cell proliferation. However, several case reports suggest that CME caused by taxanes might be due to impaired RPE function [20,25,9]. The RPE is a single layer of epithelial cells developmentally derived from the neuroectoderm and located between Bruch's membrane/choroid and the neural retina. RPE plays a pivotal role in maintaining normal retinal function by secreting nutritional factors, phagocytosing the outer segments of photoreceptors, and participating in vision formation [27]. RPE cell loss and dysfunction contribute to apoptosis and necrosis of photoreceptors, resulting in a range of retinal degeneration diseases, such as age-related macular degeneration and retinitis pigmentosa [2,15]. Therefore, in this study, we explored whether DTX has a toxic effect on RPE cells.

First, we induced differentiation of hESCs into RPE cells via EB formation to obtain hESC-RPE, which was the first hESC-derived cell type used clinically [22]. Recent advances in animal experiments and clinical studies have confirmed the value of hESC-RPE cell transplantation for treating retinal degeneration diseases [23,28,32]. Subsequently, we determined the appropriate experimental concentrations through morphological observation and cell viability assays for a better comparison with clinical applications. Morphological observation revealed that 0.3 mg/mL and higher DTX treatment resulted in a large amount of cell necrosis, a decrease in cell density, an increase in the number of particles, and a loss of normal cell shape. However, a small proportion (approximately 14%) of cells showed necrosis at 0.1 mg/mL of DTX after 24 h, and the cell viability decreased gradually over time. Thus, we selected 0.100 mg/mL DTX as the intermediate concentration for further experiments. After removing DTX, the cells were cultured in

normal culture medium, and any ongoing effects on cell morphology were observed; the DTX-induced morphological changes and damage remained and were not repaired. As such, we suspected residual DTX in the cells, potentially affecting cell growth. We found approximately 785 ng of DTX residue in the cells after treatment with 0.100 mg/mL of DTX for 48–120 h, supporting our hypothesis.

We also assessed the apoptosis, proliferation activity, and cell cycle distribution of DTX-treated cells, finding that DTX can cause significant changes in apoptosis, even at a concentration below the recommendation (0.74 mg/mL). However, we found no obvious differences among the three experimental groups, perhaps because the concentration gap was too small. As expected, DTX treatment for 24 h caused a concentration-dependent reduction in the proliferative activity of RPE cells. This situation, however, is only valid for RPE in vitro because adult human RPE cells do not normally proliferate. In healthy eyes, the RPE is a monolayer of pigmented cells that remain in the quiescent stage. RPE activation may lead to cell proliferation under pathological conditions, such as proliferative vitreoretinopathy and retinal detachment [4,16]. Additionally, in our study, the DTX-treated cells exhibited G0/G1 phase arrest and restricted cell transition into the S phase, suggesting that DTX influences cell cycle progression and, thus, restrains cell proliferation. Previous research has demonstrated that DTX induces cell cycle arrest in the G2/M phase by suppressing mitogen-activated protein kinase signaling in human renal clear cell carcinoma [14]. These differing results might be owing to distinctive cell types, drug doses, and experimental conditions. There were limitations to this study. We used hESC-RPE cells to obtain a numerical advantage since there are a limited number of adult RPE cells, and they are difficult to isolate from the patient's eyeball. However, hESC-RPE cells have a certain ability to proliferate, which adult RPE cells cannot do. Moreover, the eye has a complex structure, and various eye interactions may have different effects. The cell culture systems used in this study are incapable of mimicking the complex physiological environment of the body.

To our knowledge, this study reports for the first time that DTX directly inhibits hESC-RPE cell viability and proliferation and induces cell apoptosis and cell cycle arrest. These direct toxic effects of DTX on hESC-RPE cells may be similar to that of RPE in vivo. So far, only one

study has shown that DTX effectively blocks the migration of ARPE19 cells without affecting proliferation at non-toxic concentrations [29]. However, ARPE19 cells cannot represent RPE cells under physiological conditions. It has a low ability to express key proteins that regulate and maintain tight connections, cannot metabolize vitamin A, and has low expression of RPE markers [1]. In addition, non-toxic concentration of DTX is much lower than the level of tumor treatment and our experimental concentration. DTX in our study may affect the microtubules responsible for vesicle transport in G1 phase, resulting in cell cycle arrest and cell proliferation inhibition. We assume different concentrations of DTX will have different effects on different cells. We can speculate a likely mechanism (Fig. 6), although the detailed underlying mechanisms are still unknown. Whatever the mechanism, it is vital to evaluate the efficacy of antitumor drugs while considering their possible toxicity to healthy eye tissues.

Funding

CRediT authorship contribution statement

Zhuo Li: Conceptualization, Methodology. **Di Zhou:** Conceptualization, Methodology, Writing – review & editing. **Jialin Li:** Data curation, Writing – original draft, Visualization, Investigation, Writing – review & editing. **Xiao Liu:** Data curation, Writing – original draft. **Qiaohui Yang:** Visualization, Investigation. **Jian Huang:** Visualization, Investigation. **Wang Zhou:** Visualization, Investigation. **Zhirong Tan:** Visualization, Investigation.

Declaration of Competing Interest

The authors declare that they have no known competing financial interests or personal relationships that could have appeared to influence the work reported in this paper.

Acknowledgments

References

[1] Z. Ablonczy, M. Dahrouj, P.H. Tang, Y. Liu, K. Sambamurti, A.D. Marmorstein, C. E. Crosson, Human retinal pigment epithelium cells as functional models for the RPE in vivo, Investig. Ophthalmol. Vis. Sci. 52 (12) (2011) 8614–8620, https://doi.org/10.1167/iovs.11-8021.

[2] W.M. Al-Zamil, S.A. Yassin, Recent developments in age-related macular degeneration: a review, Clin. Interv. Aging. 12 (2017) 1313–1330, https://doi.org/10.2147/CIA.S143508.

[3] C. Albany, G. Sonpavde, Docetaxel for the treatment of bladder cancer, Expert. Opin. Investig. Drugs 24 (12) (2015) 1657–1664, https://doi.org/10.1517/13543784.2015.1109626.

[4] D.H. Anderson, W.H. Stern, S.K. Fisher, P.A. Erickson, G.A. Borgula, The onset of pigment epithelial proliferation after retinal detachment, Investig. Ophthalmol. Vis. Sci. 21 (1 Pt 1) (1981) 10–16 (https://www.ncbi.nlm.nih.gov/pubmed/7251293. PMID: 7251293).

[5] A. Banerjee, D. Das, R. Paul, S. Roy, A. Bhattacharjee, S.K. Prasad, O. Banerjee, S. Mukherjee, B.K. Maji, Altered composition of high-lipid diet may generate reactive oxygen species by disturbing the balance of antioxidant and free radicals, J. Basic Clin. Physiol. Pharmacol. 31 (3) (2020). Mar 30.

[6] A. Banerjee, D. Das, R. Paul, S. Roy, U. Das, S. Saha, S. Dey, A. Adhikary, S. Mukherjee, B.K. Maji, Mechanistic study of attenuation of monosodium glutamate mixed high lipid diet induced systemic damage in rats by Coccinia grandis, Sci. Rep. 10 (1) (2020) 15443, https://doi.org/10.1038/s41598-020-72076-6.

[7] J. Belz, N. Castilla-Ojo, S. Sridhar, R. Kumar, Radiosensitizing silica nanoparticles encapsulating docetaxel for treatment of prostate cancer, Methods Mol. Biol. 1530 (2017) 403–409, https://doi.org/10.1007/978-1-4939-6646-2_26.

[8] D. Bisacchi, R. Benelli, C. Vanzetto, N. Ferrari, F. Tosetti, A. Albini, Anti-angiogenesis and angioprevention: mechanisms, problems and perspectives, Cancer Detect. Prev. 27 (3) (2003) 229–238, https://doi.org/10.1016/s0361-090x(03)00030-8.

[9] A.M. Elhusseiny, N. Relhan, W.E. Smiddy, Docetaxel-induced maculopathy possibly potentiated by concurrent hydroxychloroquine use, Am. J. Ophthalmol. Case Rep. 16 (2019), 100560, https://doi.org/10.1016/j.ajoc.2019.100560.

[10] A. Enzsoly, K. Kammerer, J. Nemeth, M. Schneider, Bilateral cystoid macular edema following docetaxel chemotherapy in a patient with retinitis pigmentosa: a case report, BMC Ophthalmol. 15 (2015) 32, https://doi.org/10.1186/s12886-015-0020-4.

[11] B. Esmaeli, M.A. Ahmadi, E. Rivera, V. Valero, T. Hutto, D.M. Jackson, R. A. Newman, Docetaxel secretion in tears: association with lacrimal drainage obstruction, Arch. Ophthalmol. 120 (9) (2002) 1180–1182 (https://www.ncbi.nlm.nih.gov/pubmed/12215091).

[12] B. Esmaeli, V. Valero, M.A. Ahmadi, D. Booser, Canalicular stenosis secondary to docetaxel (taxotere): a newly recognized side effect, Ophthalmology 108 (5) (2001) 994–995, https://doi.org/10.1016/s0161-6420(00)00640-0.

[13] J. Folkman, Tumor angiogenesis: therapeutic implications, New Engl. J. Med. 285 (21) (1971) 1182–1186, https://doi.org/10.1056/NEJM197111182852108.

[14] T.D. Han, D.H. Shang, Y. Tian, Docetaxel enhances apoptosis and G2/M cell cycle arrest by suppressing mitogen-activated protein kinase signaling in human renal clear cell carcinoma, Genet. Mol. Res. 15 (1) (2016), https://doi.org/10.4238/gmr.15017321.

[15] D.T. Hartong, E.L. Berson, T.P. Dryja, Retinitis pigmentosa, Lancet 368 (9549) (2006) 1795–1809, https://doi.org/10.1016/s0140-6736(06)69740-7.

[16] C. Hecquet, G. Lefevre, M. Valtink, K. Engelmann, F. Mascarelli, cAMP inhibits the proliferation of retinal pigmented epithelial cells through the inhibition of ERK1/2 in a PKA-independent manner, Oncogene 21 (39) (2002) 6101–6112, https://doi.org/10.1038/sj.onc.1205765.

[17] G.N. Hortobagyi, Recent progress in the clinical development of docetaxel (Taxotere), PMID: 10426457, Semin. Oncol. 26 (3 Suppl 9) (1999) 32–36 (Retrieved from), https://www.ncbi.nlm.nih.gov/pubmed/10426457.

[18] M.W. Johnson, Etiology and treatment of macular edema, Am. J. Ophthalmol. 147 (1) (2009), https://doi.org/10.1016/j.ajo.2008.07.024.

[19] A. Kord Valeshabad, W.F. Mieler, V. Setlur, M. Thomas, M. Shahidi, Posterior segment toxicity after gemcitabine and docetaxel chemotherapy, Optom. Vis. Sci. 92 (5) (2015) e110–e113, https://doi.org/10.1097/OPX.0000000000000571.

[20] T.I. Kuznetcova, P. Cech, C.P. Herbort, The mystery of angiographically silent macular oedema due to taxanes, Int. Ophthalmol. 32 (3) (2012) 299–304, https://doi.org/10.1007/s10792-012-9558-9.

[21] S. Nghiem-Buffet, S.Y. Cohen, A. Giocanti-Auregan, Docetaxel retinopathy: a case report, Case Rep. Ophthalmol. 8 (1) (2017) 21–25, https://doi.org/10.1159/000455088.

[22] S.D. Schwartz, J.P. Hubschman, G. Heilwell, V. Franco-Cardenas, C.K. Pan, R. M. Ostrick, E. Mickunas, R. Gay, I. Klimanskaya, R. Lanza, Embryonic stem cell trials for macular degeneration: a preliminary report, Lancet 379 (9817) (2012) 713–720, https://doi.org/10.1016/S0140-6736(12)60028-2.

[23] S.D. Schwartz, C.D. Regillo, B.L. Lam, D. Eliott, P.J. Rosenfeld, N.Z. Gregori, J. P. Hubschman, J.L. Davis, G. Heilwell, M. Spirn, J. Maguire, R. Gay, J. Bateman, R. M. Ostrick, D. Morris, M. Vincent, E. Anglade, L.V. Del Priore, R. Lanza, Human embryonic stem cell-derived retinal pigment epithelium in patients with age-related macular degeneration and Stargardt's macular dystrophy: follow-up of two open-label phase 1/2 studies, Lancet 385 (9967) (2015) 509–516, https://doi.org/10.1016/S0140-6736(14)61376-3.

[24] C. Seguin, N. Kovacevich, I.A. Voutsadakis, Docetaxel-associated myalgia-arthralgia syndrome in patients with breast cancer, Breast Cancer (Dove Med Press) 9 (2017) 39–44, https://doi.org/10.2147/BCTT.S124646.

[25] C.H. Shih, Y.C. Lee, Impaired retinal pigment epithelium in paclitaxel-induced macular edema: a case report, Medicine 97 (26) (2018), e11229, https://doi.org/10.1097/MD.0000000000011229.

[26] C.A. Skolnick, D.J. Doughman, Erosive conjunctivitis and punctal stenosis secondary to docetaxel (taxotere), Eye Contact Lens 29 (2) (2003) 134–135, https://doi.org/10.1097/01.ICL.0000062464.79558.5A.

[27] O. Strauss, The retinal pigment epithelium in visual function, Physiol. Rev. 85 (3) (2005) 845–881, https://doi.org/10.1152/physrev.00021.2004.

[28] Y. Sung, M.J. Lee, M. Choi, S.Y. Jung, S.Y. Chong, J.H. Sung, S.H. Shim, W.K. Song, Long-term safety and tolerability of subretinal transplantation of embryonic stem cell-derived retinal pigment epithelium in Asian Stargardt disease patients, Br. J. Ophthalmol. 105 (6) (2021) 829–837, https://doi.org/10.1136/bjophthalmol-2020-316225.

[29] P. Tababat-Khani, L.M. Berglund, C.D. Agardh, M.F. Gomez, E. Agardh, Photocoagulation of human retinal pigment epithelial cells in vitro: evaluation of necrosis, apoptosis, cell migration, cell proliferation and expression of tissue repairing and cytoprotective genes, PLoS One 8 (8) (2013), e70465, https://doi.org/10.1371/journal.pone.0070465.

[30] B.A. Teitelbaum, D.J. Tresley, Cystic maculopathy with normal capillary permeability secondary to docetaxel, Optom. Vis. Sci. 80 (4) (2003) 277–279, https://doi.org/10.1097/00006324-200304000-00004.

[31] D.G. Telander, D. Sarraf, Cystoid macular edema with docetaxel chemotherapy and the fluid retention syndrome, Semin. Ophthalmol. 22 (3) (2007) 151–153, https://doi.org/10.1080/08820530701457373.

[32] W. Wu, Y. Zeng, Z. Li, Q. Li, H. Xu, Z.Q. Yin, Features specific to retinal pigment epithelium cells derived from three-dimensional human embryonic stem cell cultures - a new donor for cell therapy, Oncotarget 7 (16) (2016) 22819–22833, https://doi.org/10.18632/oncotarget.8185.

[33] T. Yokoe, I. Fukada, K. Kobayashi, T. Shibayama, Y. Miyagi, A. Yoshida, T. Iwase, S. Ohno, Y. Ito, Cystoid macular edema during treatment with Paclitaxel and Bevacizumab in a patient with metastatic breast cancer: a case report and literature review, Case Rep. Oncol. 10 (2) (2017) 605–612, https://doi.org/10.1159/000477897.

[34] Y. Zeng, X. Yao, X. Liu, X. He, L. Li, X. Liu, Z. Yan, J. Wu, B.M. Fu, Anti-angiogenesis triggers exosomes release from endothelial cells to promote tumor vasculogenesis, J. Extracell. Ves. 8 (1) (2019), 1629865, https://doi.org/10.1080/20013078.2019.1629865.